ISSN 8755-6839

SCIENCE OF
TSUNAMI HAZARDS

The International Journal of The Tsunami Society
Volume 27 Number 2 Published Electronically 2008

DID A SUBMARINE SLIDE TRIGGER THE 1918 PUERTO RICO TSUNAMI?

Matthew J. Hornbach[1], Steven A. Mondziel[2], Nancy R. Grindlay[2], Cliff Frohlich[1], Paul Mann[1]

For submission to *Science of Tsunami Hazards*
Corresponding author: Matthew J. Hornbach
matth@ig.utexas.edu

[1] The Institute for Geophysics, The Jackson School of Geosciences, The University of Texas at Austin, Austin, Texas, USA.

[2] University of North Carolina at Wilmington, Department of Geography and Geology. Wilmington, North Carolina, USA.

ABSTRACT

The 1918 tsunami that inundated northwest Puerto Rico with up to 6 m waves has been attributed to seafloor faulting associated with the 1918 Mona Canyon earthquake. During the earthquake a series of submarine cable breaks occurred directly off the northwest coast of Puerto Rico where the largest tsunami waves came ashore. Here, we use a recently compiled geophysical data set to reveal that a 9 km long landslide headwall exists in the region where cable breaks occurred during the 1918 earthquake. We incorporate our interpretations into a near-field tsunami wave model to evaluate whether the slide may have triggered the observed 1918 tsunami. Our analysis indicates that this slide could generate a tsunami with phase, arrival times, and run-ups similar to observations along the northwest coast of Puerto Rico. We therefore suggest that a submarine slide offers a plausible alternative explanation for generation of this large tsunami.

Introduction

Although tsunamis immediately following large earthquakes are routinely attributed to earthquake-induced seafloor faulting, submarine slides, which sometimes accompany large earthquakes, can produce destructive tsunamis [*Heinrich et al.*, 2001; *Tappin et al.*, 1999; *Tinti et al.*, 1999]. Both earthquakes and submarine slides generate tsunamis by displacing water during seafloor deformation, however, for any particular scenario of seafloor deformation (i. e., timing, source location, size, direction of motion) the resulting wave is unique [eg. *Heinrich et al., 2000; Ioualalen et al., 2006*]. By analyzing bathymetric data and earthquake fault mechanisms in tsunamigenic regions, one can constrain seafloor deformation patterns, forward-model the resulting near-field tsunamis, and identify the deformation pattern that best reproduces the observed wave.

The 1918 Puerto Rico tsunami is one of the first modern tsunami events where high-quality observations of tsunami wave phase, run-up, and arrival times were well documented, allowing for good comparison with tsunami wave models [*Mercado and McCann*, 1998; *Reid and Taber*, 1919]. Previous studies [*Mercado and McCann*, 1998] suggest that seafloor deformation caused by fault rupture of the 11 October 1918 Mw 7.3 Puerto Rico earthquake [*Engdahl and Villase–or*, 2002] generated the tsunami with wave run-up as high as 6 m along the northwest coast, that killed more than 100 people [*Reid and Taber*, 1919]. Re-analysis of the 1918 earthquake epicenter indicates that although significant (+/- 50 km) uncertainty in its exact location exists, the predicted epicenter is consistent with proposed faults that triggered the tsunami [*Doser et al.*, 2005; *Mercado and McCann*, 1998]. Analysis also indicates that the event was not a slow "tsunami earthquake," where earthquake moment magnitude is significantly larger than surface magnitude and uncharacteristically long and slow rupturing occurs [*Doser et al.*, 2005; *Kanamori and Masayuki*, 1993]. Nonetheless, surprisingly high (2-6 m) wave run-ups occurred along a localized, 15-20-km-long coastal segment of northwestern Puerto Rico between Pt. Boqueron and Pt. Higuero [*Reid and Taber*, 1919] (Figure 1).

Perhaps more importantly, however, independent evidence exists that the earthquake caused a submarine slide. Specifically, during the earthquake, multiple submarine cable breaks occurred to the northwest of Puerto Rico, just north of the epicenter [*Reid and Taber*, 1919] (Figure 1A). Cable breaks are commonly associated with submarine slides [e.g. *Krause et al.,*1970]. To date, there is no detailed bathymetric study confirming that a submarine slide occurred in this area. Here, by combining results from recently merged high-resolution seismic and bathymetric data, historical records, and a near-field tsunami model, we assess the plausibility that a submarine slide triggered the large 1918 tsunami observed along northwest coast of Puerto Rico. Using seismic and bathymetric data, we show that a large headwall exists within the cable break region, north of the Mona Canyon, and we suggest that a slide from this headwall caused the cable breaks during the 1918 earthquake and a may have triggered the tsunami.

Imaging Methods

We compiled multibeam bathymetry data from six research cruises performed over the period 1995-2004 in the northeast Mona Passage in the region of the suspected origin of the 1918 tsunami. These data sets include Atlas Hydrosweep and Seabeam 2112 multibeam bathymetry data. Recent coastal relief measurements from the northeast Mona Passage supplied by NOAA's online National

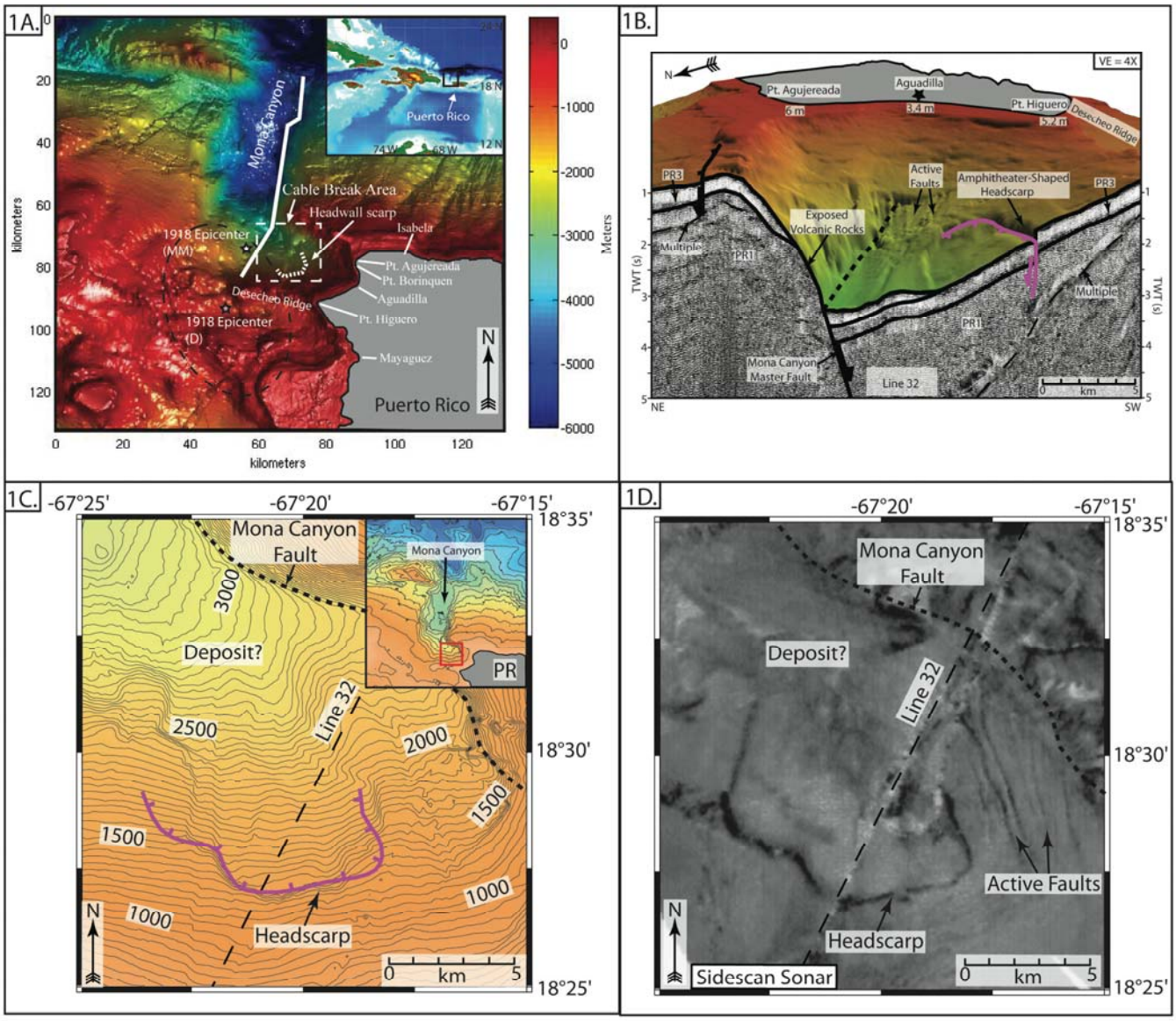

Figure 1. (A) 150 m resolution bathymetric map created from interpolating multibeam data collected along the northwest coast of Puerto Rico (inset shows regional location). The revised earthquake epicenter is south of the Mona Canyon. The dashed ellipse represents the new location of the 1918 earthquake epicenter (centered at the pink star) with 90% confidence [*Doser et al.*, 2005]. The white star represents the approximate location of the 1918 epicenter, according to *Pacheco and Sykes* [1992]. The solid white line shows the approximate location of proposed faults that may have slipped during the 1918 earthquake, suggested by *Mercado and McCann* [1998]. The dashed white box indicates the region where cable breaks occurred according to *Reid and Taber* [1919]. (B) Oblique view of seafloor and seismic line 32, collected across the cable break region and the newly discovered headscarp (pink). (C) Bathymetric data in the vicinity of the headscarp and cable break zone. (D) Sidescan sonar of the same area in (C).

Geophysical Database Center (NGDC) supplement these multibeam bathymetry data sets. All multibeam bathymetry data were processed and merged to generate a digital terrain model (DTM) of all data sets at a 150-m grid interval. We also included sidescan sonar imagery collected with the Hawaii Mapping Research (HMR) group's HMR-1 sidescan sonar system as part of research cruise EW9605. The data were slant-range and beam-angle corrected and gridded at a 17m interval. Single-channel seismic reflection data collected aboard research cruise EW9605 in the northeast Mona Passage in the suspected source region of the 1918 tsunami were processed through migration using Parallel Geoscience's Seismic Processing Workshop (SPW). We combined these data with the multibeam bathymetry and sidescan sonar data to generate pseudo three-dimensional images of the seafloor. We analyzed these data, searching for breaks in the surficial sediments indicating potential active faults, and for amphitheatre-shaped headscarps indicating the presence of submarine landslides.

Imaging Results

Multiple mass wasting features are evident in the Mona Canyon in the multibeam bathymetry, sidescan sonar, and seismic reflection data [*Grindlay et al.*, 2005; *ten Brink et al.*, 2006]. Of particular interest is a nearly semi-circular headscarp centered at 18.46^{o} north, -67.33^{o} west at ~1200 m water depth that extends ~9 kilometers northeast-to-southwest, with an average height of ~100 m, and a maximum height of ~200 m (Figure 1). This feature is approximately 18 km off the northwest coast of Aguadilla, Puerto Rico and is located in the same region as two submarine cable breaks documented by *Reid and Taber* [1919]. However, because the available seismic sections are widely spaced the exact limits of the downslope slide deposit remain poorly known. From the shape and length of the headwall (a semi-circular feature approximately ~9 km long and ~100 m high), we estimate that the maximum slide volume, assuming this was a single contiguous slide event, is no greater than ~6 km^{3}.

We propose that the 11 October 1918 M_{W} 7.3 earthquake re-activated motion along the antithetic (east-dipping) fault on the hanging wall of the southern Mona Canyon half-graben (north of Desecheo Ridge) (Figure 1B). We proposed that seafloor rupture of this fault triggered a slope failure that subsequently broke the submarine cables as it traversed down slope, displaced the water column, and generated the 2-6 m-high tsunami that inundated the northwest coast of Puerto Rico.

Comparison of Imaging Results with Historic Observations

Our observations are in excellent agreement with more limited observations made by ocean bottom cable surveyors, who studied the bathymetry in the cable-break region immediately following the earthquake. Specifically, the captain of the cable repair ship noted that depth soundings obtained during cable repair indicated an apparent increase in depth of as much as183 meters in the cable break area, although relatively poor navigation might also explain this discrepancy [*Reid and Taber*, 1919]. Perhaps more revealing, however, is that the cable repair crew found long sections ("two-to-three miles") of cable crushed and buried underneath sediment in this region [*Reid and Taber*, 1919]. The correlation of the bathymetric study results with the cable repair observations strongly suggest that a kilometer-scale submarine slide occurred in this vicinity during the 1918 earthquake.

Submarine Slide Modeling

We used seafloor bathymetric data combined with previously published submarine slide models to estimate slide motion. The bathymetric data fix the location of the headwall and the slope of the seafloor, and we use these parameters to constrain slide size, direction, and velocity. To estimate of slide size, we assume it had a maximum width and height of 9 and 0.2 km, respectively. These are maximum values, since it is possible that only a portion of the headwall failed, and that the headwall potentially formed piecemeal during multiple individual slide events. The length of the slide is difficult to determine, and would require a high resolution coring and seismic study to constrain fully. Given the roughly symmetric, scalloped-shaped headwall, we here assume a symmetric slide, and model it as a 2D Gaussian function with a diameter (2-sigma) of 9 km and a maximum height of 200 m, resulting in a maximum slide volume of ~6 km^3. As noted in previous tsunami modeling studies [*Ward*, 2001], an increase/decrease in slide volume will result in a corresponding increase/decrease in tsunami wave height. For a first-order model of slide motion, we assume the slide accelerates uniformly down-slope, consistent with submarine slide modeling and experiments [*Grilli and Watts*, 1999; *Watts*, 1997], and we also assume a seafloor slope of 7¡ a mean slide direction of ~305¡E of N, both estimated from bathymetric data. It remains unclear from the bathymetric data how far the slide transports material down slope and where break-up occurs; given that no clearly identifiable large slide blocks exist down slope with this event, we suggest that as the slide accelerated down slope, it gradually broke-up, dispersed, and distributed debris over a large area. Previous slide tsunami modeling studies show that slide deceleration and evolution have only second order effects on tsunami wave development [*Jiang and LeBlond*, 1992; *Watts et al.*, 2005], and we therefore assume that slide initiation generates the primary tsunami wave. Indirect measurements of slide velocities from the timing and location of cable breaks at other known slides indicate that the group velocity of slide material likely does not exceed 30-40 m/s [e.g. *Krause et al.,1970*], and therefore, we limit terminal slide velocity to 40 m/s.

Tsunami Modeling

We use a standard hydrostatic non-linear long wave model to characterize the tsunami generated by the submarine slide [eg. *Heinrich et al.*, 2000; *Tinti et al.*, 1999]. Because the tsunami source area is close (<25 km) to where the near-field wave impacts shore, the finite-difference code incorporates a non-dispersive leap-frog wave propagation technique to model the wave through time and incorporates both Coriolis and frictional forces. For bathymetry, we use the previously described bathymetric data collected from multibeam surveys, gridded at 150 m intervals, with a total model domain of 680 square cells.

The wave propagation model enables us to assess wave phase, arrival times, and wave run-up for the slide-generated near-field tsunami. Although far-field tsunami waves were recorded during this tsunami event (with the most distant wave detected via tide-gauges along the US east coast [*Reid and Taber*, 1919]), analysis of this far-field data requires a much larger high-resolution grid than we currently have, and such an analysis goes beyond the scope of the this data set, this model, and this study. Although near-field wave phase, arrival times, and run up can all be accurately determined using this tsunami model, wave run-up will have the greatest error due to (1) shoreline bathymetric

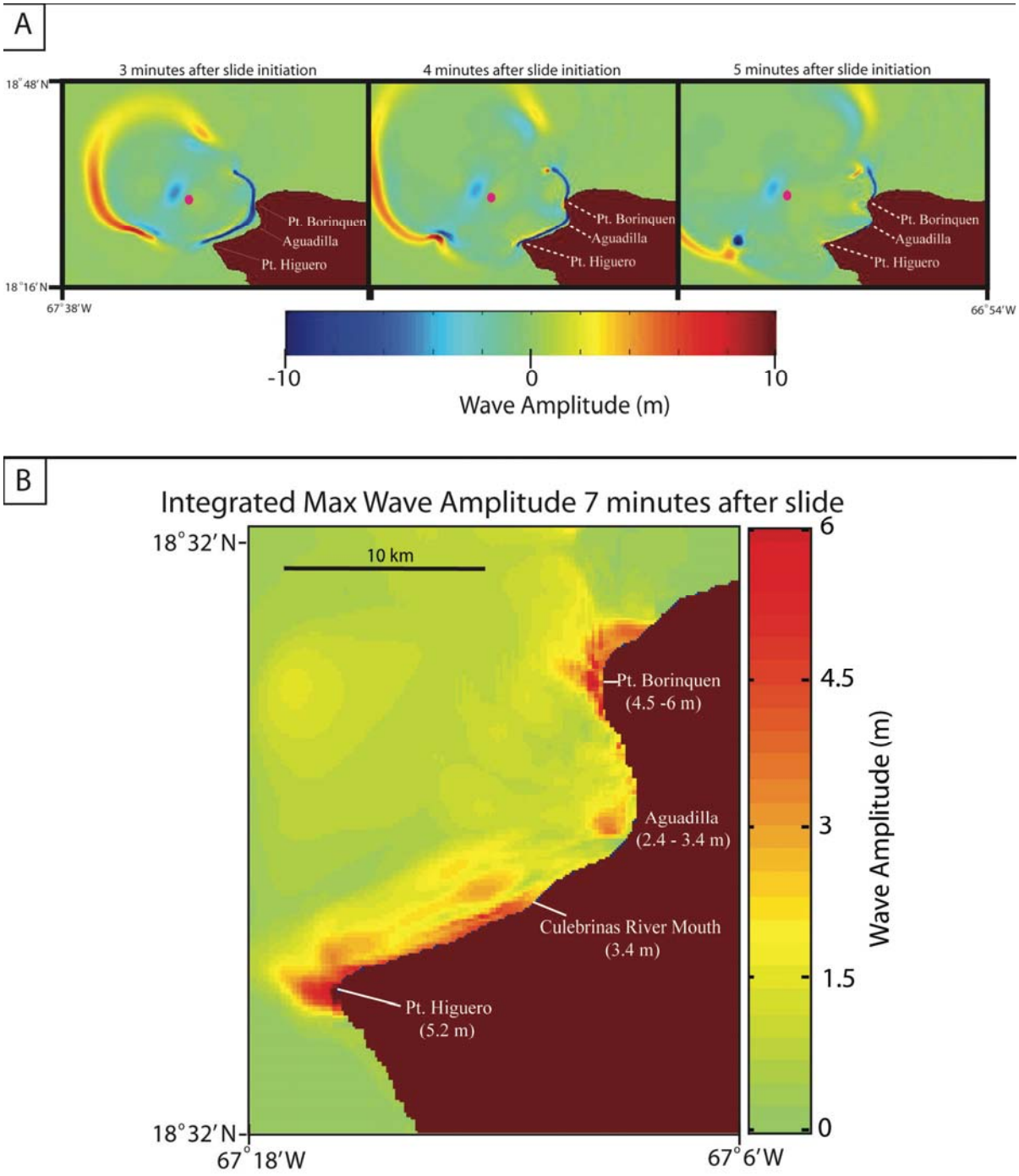

Figure 2. (A) Model results for a tsunami wave generated by a 6 km^3 slide showing the projected wave propagation pattern 3, 4, and 5 minutes after slide initiation. Wave amplitudes are in meters. The model shows a negative polarity wave initially arrives along the northwest coast of Puerto Rico, first at Pt. Borinquen, followed by Pt. Higuero and Aguadilla, consistent with first hand accounts (see Table 1). The pink dot represents the approximate location of the slide center at these time intervals. (B) Modeled wave amplitudes observed during the first 7 minutes of wave propagation for a 6 km^3 slide, with the highest wave amplitudes in red and the lowest in light green. Locations where known wave run-up values exist are also noted. In general, wave run-ups are consistent with observations (see Table 1).

resolution being limited to 150 m, and (2) limited constraints on the exact volume of the slide. By modeling what we believe is the largest slide that likely occurred (~6 km^3), we place an upper limit on run-up, since all else being equal, the larger the slide, the larger the wave [e.g. *Ward*, 2001]. To estimate possible error caused by bathymetry, we compare run-up values at multiple adjacent grid points, and use these difference to note potential run-up variability. To place constraints on the effect slide volume has on run-up, we also ran an additional model in which the height of the slide is reduced by half, resulting in a volume reduction of approximately 3 km^3.

Tsunami Model Results

We focus our results on calculated wave arrival times, phase, and run-up for the near-field tsunami wave at Pt. Borinquen, Pt. Higuero, Aguadilla, the three closest locations to the 6 km^3 slide, and the only locations impacted by the near-field tsunami where excellent observations of wave arrival times, wave phase, and run-up exist. Our analysis shows that the wave arrives first at Pt. Borinquen, 2.5-3.0 minutes after slide initiation, second at Pt. Higuero, ~3.5-4.0 minutes after slide initiation, and finally, at Aquadilla, 4.5-5.0 minutes after slide initiation (See Figure 2, and Table 1). At all locations, the initial arriving wave has a negative-to-positive phase. Wave run-up values indicate that the largest waves approaches Pt. Higuero (4.4 m +/- 1.7 m) and Pt. Borinquen (4.5 +/- 1 m), and finally Aguadilla (2.3 +/- 1.2 m) (Figure 2B, and Table 1). Similarly, model results for the 3 km^3 slide produced nearly identical wave arrival times, phase, and relative wave run-ups, however, absolute run-ups were reduced by ~60% compared to the 6 km^3 slide (Table 1).

Table 1. Comparison of observed vs. modeled amplitude, phase and arrival times

Location	Observed wave arrival time (min)	Modeled arrival time (min)	Observed phase	Modeled phase	Observed max wave run-up (m)	Modeled run-up for 6 km^3 slide and error (1 sigma) (m)	Modeled run-up for 3 km^3 slide and error (1 sigma) (m)
Pt. Borinquen	0 - 3	2.5 - 3	neg/pos	neg/pos	4.5 - 6	4.4 (+/-1.7)	2.0 (+/- 1.3)
Aguadilla	4 - 7	4.5 - 5	neg/pos	neg/pos	2.4 - 3.4	2.3 (+/-1.2)	0.9 (+/- 0.4)
Pt. Higuero	>3	3.5 - 4	neg/pos	neg/pos	5.2	4.5 (+/-1.0)	1.7 (+/- 0.4)

Did a slide trigger the 1918 Puerto Rico tsunami?

The modeled arrival times, wave phase, and run-ups generated by the slide are in good agreement with direct observations. The model indicates that a negative phase (ocean withdrawal) first arrives along the northwest coast of Puerto Rico (Figure 2A). Observers along the northwest corner of the island reported that the ocean drew-down several meters before inundating the coast a few minutes later, identical to model predictions.

Wave arrival times along the northwest coast of Puerto Rico also match observations, with the wave first arriving at Pt. Borinquen, followed by Pt. Higuero, Aguadilla. (Figure 2A, Table 1).

According to first-hand accounts, the shaking from the earthquake along the northwest coast lasted 2-3 minutes [*Reid and Taber*, 1919]. Assuming the slide occurred during the earthquake, wave arrival times are consistent with observations. For example, at Pt. Borinquen, ocean retreat was observed by the lighthouse keeper within three minutes and during the time of earthquake shaking [*Reid and Taber*, 1919], as predicted by our model. Likewise, the lighthouse keeper at Pt. Higuero observed the wave approach shore "shortly after" the earthquake, indicating that the wave likely arrived just after three minutes, also consistent with model results [*Reid and Taber*, 1919]. At Aguadilla, recorded wave arrival times range from four to seven minutes, and also match the 5 minute arrival time predicted by the model.

Model results for wave run-up assuming a 6 km^3 slide are also consistent with observations, with the largest run-ups observed at the Pts. Higuero and Borinquen followed by Aguadilla. High-water mark measurements along the northwest coast of Puerto Rico following the 1918 event suggest that the largest waves came ashore in the regions of Pt. Borinquen and Pt. Higuero, followed by the Aguadilla region, [*Reid and Taber*, 1919] (see Table 1 and Figure 2B). Furthermore, modeled wave run-up values for the 6 km^3 slide closely match observations and indicate that such a slide could generate the appropriate sized waves (Table 1).

To test the effect of slide size on wave run-up, we ran an additional model in which we reduced slide volume by 50%. This model resulted in nearly identical arrival times and phase with the original model, however, predicted wave run-up values were reduced on average by ~60% (Table 1), thereby indicating that a smaller slide may not be able to reproduce observed wave run-up values. Thus, we suggest that most if not all of the slide headwall must have failed to generate the observed near-field waves.

In spite of the relative simplicity of the slide model, which makes basic assumptions of slide shape, size and motion, the model replicates near-field observations of arrival time, phase, and run-up with considerable accuracy. The greatest errors in the model involve predicted run-up, as expected with a model where slide volume, local topography, and human factors (such as building locations and agricultural development zones) have a significant impact on run-up. Therefore, some discrepancy between predicted versus observed run-up is expected, provided first order estimates are generally consistent with observations.

Additional support for the slide triggering the tsunami is the strong evidence that a large slide occurred during the earthquake, i. e., the existence of multiple cable breaks and kilometer-length regions of buried cable in the vicinity of a well-imaged slide headwall. Whether this slide represents the primary source of the tsunami remains debatable. The fact that a submarine slide tsunami model generates a near-field wave with the appropriate arrival times, phase, and run-up along the northwest corner of Puerto Rico offers a compelling case that the slide may have played a key role in triggering the near-field portion of the 1918 tsunami, however, a more detailed study of the far-field wave is ultimately needed to determine if a slide can explain more distant tsunami observations. The occurrence of a concentrated wave run-up zone along the northwest coast of Puerto Rico, adjacent to the slide, is consistent with other near-field slide generated tsunami sources [e.g. *Heinrich et al.,* 2001*, Tappin et al.,* 1999]. Furthermore, the slide volume, which we estimate from bathymetry ranged between 2-6 km^3, is comparable in size with the 4 km^3 1998 Papua New Guinea slide that also generated a devastating yet regionally focused tsunami [*Heinrich et al.*, 2001; *Tappin et al.*, 1999].

The case for a submarine slide triggering the 1918 tsunami is compelling but equivocal. Not all slides generate tsunami, as noted by the fact that an aftershock 13 days after the 11 October 1918 earthquake triggered a second submarine slide that again broke cables in the same vicinity, yet no observed tsunami was reported [*Reid and Taber*, 1919]. Further analysis using higher resolution data over a greater modeling domain would be valuable. Some of the far-field tsunami run-up observations for the 1918 event, including those made in the Dominican Republic and Virgin Islands as well as the east coast of the US [*Reid and Taber*, 1919], may be difficult to reconcile with a slide-only scenario, since it seems counterintuitive that such a small slide could trigger a tsunami detected several thousands of kilometers away. Detailed analysis of these far-field observations requires further study that goes beyond the scope of this work.

Conclusions

Newly merged bathymetric and seismic data reveal a seafloor slide in the vicinity where multiple cable breaks occurred off the northwest coast of Puerto Rico during the 1918 earthquake. Comparison of near-field tsunami modeling results for this slide with historic observations of the tsunami produces a generally consistent match, and we suggest that a slide-generated tsunami in the cable-break region offers a viable alternative explanation for the observed near-field 1918 Puerto Rico tsunami. Submarine slide scarps are ubiquitous not only along Puerto Rico [*Grindlay et al.*, 2005; *ten Brink et al.*, 2006], but most continental margins including the Pacific Rim and Caribbean, where steep slopes exist and large tsunami occur frequently. Given that submarine slides are oftentimes triggered by earthquakes in these regions [*Meuneir et al.*, 2007], we postulate that they are perhaps more frequent tsunami generators than is commonly assumed. Our analysis highlights how high-resolution multibeam data coupled with side-scan sonar and seismic images can improve our understanding of earthquake-induced seafloor deformation, submarine sliding, and the tsunami generation. Future seismic analysis in the vicinity of the slide would place better constraints on slide volume and timing. Obtaining higher resolution bathymetric data over a broader region for far-field tsunami analysis, combined with coring and dating of slide debris would also help assess whether this slide ultimately triggered the 1918 tsunami.

Acknowledgements

We thank D. Doser for helpful conversations regarding character of the 1918 earthquake. This work was supported by NSF#OCE-9796189, UPR SeaGrant # R-122-1-04, UNCW's Center for Marine Science and Department of Geography and Geology, and the Geology Foundation at The University of Texas, Jackson School of Geosciences.

References:

Doser, D., et al. (2005), Historical earthquakes of the Puerto Rico--Virgin Islands region, in *Active tectonics and seismic hazards of Puerto Rico, the Virgin Islands, and offshore areas: Geological Society of America Special Paper 385*, edited by P. Mann, pp. 103-114, Geological Society of America.

Grilli, S. T., and P. Watts (1999), Modeling of waves generated by a moving submerged body. Applications to underwater landslides, *Engineering Analysis with Boundary Elements*, *23*, 645-656.

Grindlay, N. R., et al. (2005), A High Risk of Tsunami in the Northern Caribbean, *Eos*, *86*(12), 121,124.

Heinrich, P., et al. (2000), Near-field modeling of the July 17, 1998 tsunami in Papua New Guinea, *Geophys. Res. Let.*, *27*(19), 3037-3040.

Heinrich, P., et al. (2001), Numerical modelling of tsunami generation and propagation from submarine slumps: the 1998 Papua New Guinea event, *Geophys. J. Int.*, *145*, 97-111.

Ioualalen, M., et al. (2006), Numerical modeling of the 26 November 1999 Vanuatu tsunami, *J. Geophys. Res.*, *111*.

Jiang, L., and P. H. LeBlond (1992), The coupling of a submarine slide and the surface wave which it generates, *J. Geophys. Res.*, *97*(C8), 12731-12744.

Kanamori, H., and K. Masayuki (1993), The 1992 Nicaragua earthquake: a slow tsunami earthquake associated with subductioned sediments, *Nature*, *361*, 714-716.

Krause, D. C., et al. (1970), Turbidity currents and cable breaks in the western New Britain trench, *Geol. Soc. Amer. Bull.*, *81*, 2153-2160.

Mercado, A., and W. McCann (1998), Numerical Simulation of the 1918 Puerto Rico Tsunami, *Natural Hazards*, *18*, 57-76.

Meunier, P., N. Hovius, and A. J. Haines (2007), Regional patterns of earthquake-triggered landslides and their relation to ground motion, *Geophy. Res. Let.,34*(L20408)

Pacheco, J. F., and L. R. Sykes (1992), Seismic Moment Catalog of Large Shallow Earthquakes, 1900 to 1989, *Bull. Seismol. Soc. Amer.*, 82(3), 1306-1349

Reid, H. F., and S. Taber (1919), The Porto Rico earthquakes of October-November 1918, *Bull. Seismol. Soc. Amer.*, *9*(4), 94-127.

Tappin, D. R., et al. (1999), Sediment slump likely caused 1998 Papua New Guinea tsunami, *EOS*, *80*(30), 329,334,340.

ten Brink, U. S., et al. (2006), Size distribution of submarine landslides and its implication to tsunami hazard in Puerto Rico, *Geophys. Res. Let.*, *33*(L11307).

Tinti, S., et al. (1999), Numerical simulation of the landslide-induced tsunami of 1988 on Vulcano Island, Italy, *Bull. Volcanology*, *61*, 121-137.

Ward, S. N. (2001), Landslide tsunami, *J. Geophys. Res.*, *106*(6), 11201-11215.

Watts, P. (1997), Water waves generated by underwater landslides, California Institute of Technology, Pasadena. Ph.D Thesis

Watts, P., et al. (2005), Tsunami generation by submarine mass failure. II: Predictive equations and case studies, *J. of Waterway, Port, Coastal, and Ocean Engineering*, *131*(6), 298-310.